

Submillimetre observations of luminous $z > 4$ radio-quiet quasars and the contribution of AGN to the submm source population

Richard G. McMahon¹, Robert S. Priddey¹, Alain Omont², Ignas Snellen¹,
Stafford Withington³

1. *Institute of Astronomy, Madingley Road, Cambridge CB3 0HA, UK*

2. *Institut d'Astrophysique de Paris, CNRS, 98 bis Bd. Arago, F-75014, Paris, France*

3. *Mullard Radio Astronomy Observatory, Cavendish Laboratory, Cambridge CB3 0HE, UK*

email: rgm, rpriddey@ast.cam.ac.uk, omont@iap.fr, snellen@ast.cam.ac.uk, stafford@mrao.phys.ast.cam.ac.uk

Accepted 1999 June 29

ABSTRACT

We present sensitive 850 μm SCUBA photometry of a statistically-complete sample of six of the most luminous ($M_B < -27.5$; $\nu L_\nu(1450 \text{ \AA}) \gtrsim 10^{13} L_\odot$), $z > 4$ radio-quiet quasars, reaching noise levels ($1\sigma \sim 1.5 \text{ mJy}$) comparable with the deep blank sky surveys. These observations probe the rest frame far infrared region ($\sim 150 \mu\text{m}$), at luminosity levels for thermal sources comparable with those that *IRAS* permitted for low redshift quasars. One quasar (BR2237–0607; $z = 4.55$) is detected at 850 μm with a flux of $5.0 \pm 1.1 \text{ mJy}$ (4.5σ), whilst a second (BR0019–1522; $z=4.52$) has a detection at the 2σ level. When combined with our previous millimetre measurements of $z > 4$ quasars, we find that there is a large range (5–10) in far infrared (FIR) luminosity (L_{FIR}) at fixed UV luminosity, and that the typical quasar has a L_{FIR} and mass of cool (50 K) dust similar to that of the archetypal low redshift ($z=0.018$) ultraluminous *IRAS* galaxy (ULIRG) Arp220 ($L_{\text{FIR}} \sim 5 \times 10^{12} L_\odot$; $M_{\text{d}}(\text{cool}) \sim 10^8 M_\odot$). If one assumes a fiducial FIR luminosity of $5 \times 10^{12} L_\odot$ for all quasars with $M_B < -23$, we find that $\gtrsim 15$ per cent of the sources in the SCUBA deep surveys could be classical broad-lined radio-quiet AGN. Thus if one considers the observed ratio of Seyfert II to Seyfert I galaxies at low redshift and any contribution from totally optically obscured AGN, a significant fraction of the SCUBA source population will harbour AGN and hence the inferred star formation rates from submm fluxes may be overestimated if the active nuclei are bolometrically dominant or the IMF is top heavy.

Key words:

quasars: general – quasars: individual BR2237–0607 – cosmology: observations – galaxies: starburst – infrared: galaxies – ISM: dust

1 INTRODUCTION

Recent deep SCUBA surveys (Smail, Ivison & Blain 1997; Hughes et al. 1998; Barger et al. 1998; Eales et al. 1998) have revealed a significant population of discrete submillimetre sources, amounting to $\sim 1000 \text{ deg}^{-2}$ above $\sim 3 \text{ mJy}$ at 850 μm . If these objects lie at redshifts greater than 1, they have a far infrared (FIR) luminosity $L_{\text{FIR}} \sim 10^{12-13} L_\odot$, assuming a dust temperature of $\sim 50 \text{ K}$. Since the large negative K -correction of the dust thermal spectrum means that for $1 \lesssim z \lesssim 10$, this luminosity is insensitive to source redshift (*cf.* Arp220 in Figure 1). Prior to the SCUBA surveys, the only significant known high redshift population with comparable bolometric luminosity were the quasars. However,

the characterisation of the FIR properties of the high redshift quasars is rather meagre. Following the first detections of rest frame FIR emission from $z > 3$ radio quiet quasars (McMahon et al. 1994), our current knowledge is still biased towards more luminous objects with 850 μm fluxes in the $\sim 10\text{--}50 \text{ mJy}$ range (Isaak et al. 1994; McMahon et al. 1994; Omont et al. 1996a).

The onset of nuclear activity seems to be closely connected with significant structure-formation events. At high redshift, black holes form in rare overdense regions and are fuelled by their collapsing host objects (Haehnelt & Rees 1993); at low redshifts, interactions/mergers provoke inflow of gas to the galactic nuclei (Barnes & Hernquist 1996), fuelling central black holes. These processes would be expected

Table 1. Program objects, observing conditions and results.

| Object name | z | M_B | $S_{1.4\text{ GHz}}$ (3σ) | $R_{8.4}$ | t_{int} (mins) | $\tau_{225\text{ GHz}}$ (mean) | $\tau_{850\mu\text{m}}$ | $\tau_{450\mu\text{m}}$ | F_{850} (mJy) | F_{450} (mJy) |
|----------------|------|-------|---------------------------------------|-----------|----------------------------|-----------------------------------|-------------------------|-------------------------|--------------------|--------------------|
| BR B0019–1522 | 4.52 | –27.6 | $<0.5^1$ | <2 | 108 | 0.08 | 0.21–0.26 | 1.1–2.4 | 3.3 ± 1.6 | 11 ± 33 |
| PSS J0134+3307 | 4.52 | –28.2 | $<1.5^2$ | <3 | 108 | 0.08 | 0.27–0.34 | 1.8–2.5 | 0.4 ± 1.5 | -3 ± 54 |
| PSS J0248+1802 | 4.43 | –27.9 | $<1.5^2$ | <5 | 36 | 0.10 | 0.23–0.46 | 2.4–3.2 | 6.4 ± 4.5 | -433 ± 264 |
| PSS J0747+4434 | 4.42 | –28.2 | $<0.5^3$ | <5 | 54 | 0.08 | 0.27–0.39 | 1.8–2.5 | 0.0 ± 2.2 | 72 ± 105 |
| BR B1600+0729 | 4.35 | –28.1 | $<0.5^1$ | <2 | 108 | 0.09 | 0.28–0.33 | 1.7–2.0 | 1.8 ± 1.6 | -7 ± 55 |
| BR B2237–0607 | 4.55 | –28.1 | $<0.5^1$ | <5 | 144 | 0.07 | 0.29–0.41 | 1.8–2.7 | 5.0 ± 1.1 | 19 ± 53 |

Notes: Radio flux limits taken from (1) McMahon et al, in preparation; (2) Condon et al, 1998; (3) Becker et al, 1995

to trigger a major starburst, though the relative prominence of either component, starburst or AGN, would depend on the precise dynamical details of the collapse or interaction.

In this paper, we report SCUBA 850 μm photometry of a statistically complete sample of six of the most luminous, $z > 4$, radio-quiet quasars. Our previous work at 800 μm with the JCMT (Isaak et al. 1994) and 1.25 mm with the IRAM 30 m (McMahon et al. 1994, Omont et al. 1996a) and was only sensitive to relatively high luminosity sources. The aim of the current work is to carry out more sensitive observations of a small sample of radio quiet quasars in an effort to make an initial estimate of the contribution of AGN at high redshift to the submillimetre source population.

Unless stated otherwise, we assume $H_0 = h_{50} \times 50 \text{ km s}^{-1} \text{ Mpc}^{-1}$ and $q_0 = 0.5$ throughout this paper.

2 OBSERVATIONS

The quasars for study were selected from the APM samples of high redshift quasars (Storrie-Lombardi et al. 1996, McMahon et al. in prep.) and PSS survey (Kennefick et al. 1995). From extant radio data as tabulated in Table 1, the quasars are radio quiet based on the definition, $\text{Log } R_{8.4} < 1.0$, where $R_{8.4} = L_{8.4}/L_B$, is the ratio of radio and optical luminosities as defined by Hooper et al (1996), where spectral indices of -0.5 and -0.7 have been used to extrapolate to the rest frame optical and radio fluxes. Moreover, based on the observed median spectral index of -0.7 found for radio loud quasars over the wavelength range, the expected contamination at 850 μm is $<0.1 \text{ mJy}$ in all cases. The most luminous $z > 4$ objects were selected in the HA range 15–08 as determined by the telescope scheduling, providing effectively sparse sampling for $M_B < -27.5$.

Observations were carried out during three 8 hr observing shifts over the period 1998 August 16 to 19, with the Submillimetre Common-User Bolometer Array (SCUBA) (Holland et al. 1998) on the 15 m James Clerk Maxwell Telescope. We used SCUBA in standard point-source photometry mode at 450 and 850 μm . This involves placing the target on the central bolometer of each array, whilst ‘jiggling’ the secondary mirror in a 9-point pattern with 2 arcsec offsets, integrating for 1 second at each. Superimposed on this is a chop of the secondary mirror by 60 arcsec (in azimuth) at 7 Hz, to remove sky emission; after the first 9-point jiggle, the telescope is nodded such that the chop position lies on the opposite side of the source. Uranus was used as the primary flux calibrator. Skydips were taken regularly to deter-

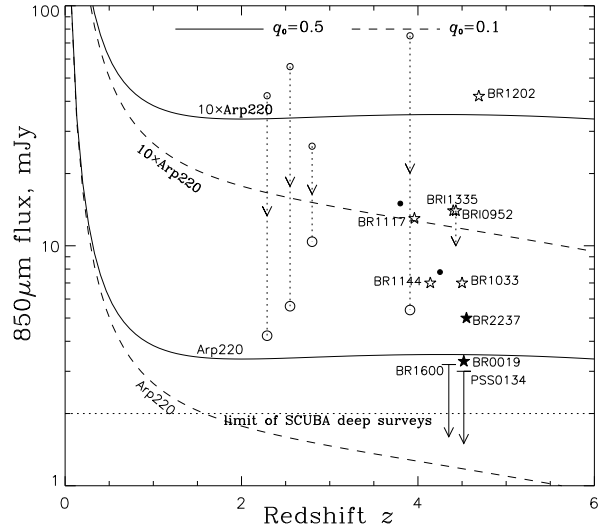


Figure 1. The current status of the high redshift ($z > 1$) 850 μm Hubble diagram using the observations presented in Table 2. Radio galaxies are shown as filled circles; open circles show the submm detected lensed sources with vertical lines connecting the observed flux with the unlensed fluxes; open stars show previously detected radio quiet $z > 4$ quasars; filled stars show our new observations. Upper limits are plotted at the 2σ limit with arrow length equal to the 1σ uncertainty. Also plotted is the expected flux from a thermal source like Arp220 as function of redshift for two cosmologies using the observed SED from Klaas et al. (1997).

mine the sky opacity which varied considerably throughout the run as reported in Table 1.

Data reduction was performed with the Starlink `SURF` software, and consisted primarily of experimenting with sky-removal techniques, using the mean and median of different rings of bolometers as a background estimates. The results were robust to variations in the precise method, and we take the ‘mean-of-the-innermost-ring’ as our standard sky value.

3 RESULTS

At 850 μm , one quasar, BR2237–0607 at $z = 4.55$, is detected with high significance (4.5σ), while the quasar BR0019–1522 has a detection at 2σ . Two of the remaining objects have good $1\sigma \approx 1.5 \text{ mJy}$ upper limits. None of the objects are detected at 450 μm ; at this wavelength, the

Table 2. Physical properties of representative 850 μm sources, assuming $T_d = 50\text{ K}$ and $\beta = 1.5$

| Object name | | Redshift z | F_{850} (mJy) | M_d ($h_{50}^{-2} 10^8 M_\odot$) | L_{FIR}^\dagger ($h_{50}^{-2} 10^{12} L_\odot$) | SFR ($\alpha \times h_{50}^{-2} M_\odot \text{ yr}^{-1}$) | M_B^\ddagger |
|------------------------------|--------------|-----------------|----------------------|---|---|--|----------------|
| BR0019–1522 | Quasar | 4.52 | 3.3 ± 1.6^1 | 1.5 ± 0.7 | 5.0 ± 2.4 | 500 | –27.6 |
| PSS0134+3307 | Quasar | 4.52 | $< 3.0^1$ | < 1.4 | < 4.5 | < 450 | –28.2 |
| BR1600+0729 | Quasar | 4.35 | $< 3.2^1$ | < 1.5 | < 4.9 | < 490 | –28.1 |
| BR2237–0607 | Quasar | 4.55 | 5.0 ± 1.1^1 | 2.3 ± 0.5 | 7.5 ± 1.6 | 750 | –28.1 |
| BRI0952–0115 ^{l,a} | Quasar | 4.43 | 14 ± 2^2 | 6.5 ± 0.9 | 21.2 ± 3.0 | 2120 | –27.7 |
| BR1033–0327 | Quasar | 4.50 | 7 ± 2^2 | 3.2 ± 0.9 | 10.5 ± 3.0 | 1050 | –27.6 |
| BR1117–1329 | Quasar | 3.96 | 13 ± 1^2 | 6.4 ± 0.5 | 20.8 ± 1.6 | 2080 | –28.1 |
| BR1144–0723 | Quasar | 4.14 | 7 ± 2^2 | 3.4 ± 1.0 | 11.0 ± 3.1 | 1100 | –27.5 |
| BR1202–0725 | Quasar | 4.69 | 42 ± 2^2 | 19.0 ± 0.9 | 62.0 ± 3.0 | 6200 | –28.5 |
| BRI1335–0417 | Quasar | 4.40 | 14 ± 1^2 | 6.5 ± 0.5 | 21.3 ± 1.5 | 2130 | –27.3 |
| 8C1435+635 | Radio Galaxy | 4.25 | 7.77 ± 0.76^3 | 3.7 ± 0.4 | 12.0 ± 1.2 | 1200 | –24.4 |
| 4C41.17 | Radio Galaxy | 3.80 | $17.4 \pm 3.1^{4,m}$ | 7.5 ± 1.3 | 24.5 ± 4.4 | 2450 | –25.0 |
| APM08279+5255 ^{l,b} | Quasar | 3.91 | 75 ± 4^5 | 2.6 ± 0.1 | 8.6 ± 0.5 | 860 | –31.0 |
| SMM02399–0136 ^{l,c} | Seyfert 2 | 2.80 | 26 ± 3^6 | 6.1 ± 0.7 | 19.8 ± 2.3 | 1980 | –24.0 |
| H1413+117 ^{l,d} | Quasar | 2.55 | $66 \pm 7^{7,m}$ | 3.4 ± 0.4 | 11.1 ± 1.2 | 1110 | –28.5 |
| F10214+4724 ^{l,e} | Seyfert 2 | 2.29 | $50 \pm 5^{8,m}$ | 0.9 ± 0.1 | 2.9 ± 0.3 | 290 | –23.1 |
| Arp220 | Starburst | 0.0183 | $67000^{9,n}$ | 1.7 | 5.5 | 550 | –21.3 |

Notes: \dagger The uncertainty only reflects the flux uncertainty. \ddagger Computed from observed optical continuum magnitudes assuming a spectral index of -0.5 , except in the cases of the radio galaxies, where K -band magnitudes were used. ^lLensed objects. Magnification factors for the FIR continuum are (a) uncertain; (b) 10 (Green & Rowan-Robinson, 1999; see also Downes et al. 1995); (c) 2.5 (Ivion et al., 1998b), (d) 10 (Yun et al., 1997), (e) 30 (Eisenhardt et al. 1996). Derived physical quantities are corrected by these factors.

^m800 μm fluxes; equivalent 850 μm fluxes would be 15, 56 and 42 mJy, respectively. ⁿISO 170 μm flux (*N.B.*, at $z \sim 4$, 850 μm corresponds to a rest wavelength of $\sim 170\ \mu\text{m}$).

References: 1. This work; 2. Buffey et al. (in prep.); 3. Ivison et al. (1998a); 4. Dunlop et al. (1994); 5. Lewis et al. (1998); 6. Ivison et al. (1998b); 7. Hughes et al. (1997); 8. Rowan-Robinson et al. (1993); 9. Klaas et al. (1997).

observations are noisy, because weather was on the whole unfavourable, so we disregard data in this band. Our observed fluxes are compared with those of other cosmological submillimetre sources in Figure 1.

We can derive dust masses and FIR luminosities from our observations as described in more detail in McMahon et al. (1994). There is considerable uncertainty in these procedures (*e.g.* Figure 2), but we can assume physical parameters derived for better-studied objects and extrapolate from our 850 μm measurements. The mass of a dust cloud optically thin in the FIR is given by

$$M_d = \frac{S_\nu(\nu_{\text{obs}}) D_L^2}{\kappa_d B_\nu(\nu_{\text{rest}}, T_d) (1+z)}, \quad (1)$$

where D_L is the luminosity distance and κ_d is the absorption coefficient:

$$\kappa_d = \kappa_{850} \times \left(\frac{\nu_{\text{rest}}}{353\text{ GHz}} \right)^\beta. \quad (2)$$

We assume a frequency dependence of absorption coefficient of $\beta = 1.5$, as shown to be a good fit for both low redshift luminous infrared galaxies (Carico et al., 1992) and luminous high redshift quasars (Benford et al., in prep.) and $\kappa_{850} = 0.11\text{ m}^2\text{ kg}^{-1}$, based on the widely-used Hildebrand (1983) normalisation at 125 μm ($\kappa = 1.875\text{ m}^2/\text{kg}$), which we have extrapolated to longer rest wavelengths assuming $\beta=1.5$.

The above assumes that the rest-frame FIR continuum is thermal emission from dust which is optically thin to FIR photons, which is justified since spectral indices in the Rayleigh-Jeans region for typical $z > 4$ quasars are $\gtrsim 3$

(Buffey et al. in prep., Isaak et al., 1994). It also assumes that the dust is isothermal: a single temperature of 50 K is a typical value derived from fits to well-covered FIR SEDs. If the dust were not isothermal, fits to the currently-available data would be biased towards the higher temperatures, causing us to underestimate the true dust mass. *ISO* Photometry of nearby ULIRGs (Klaas et al. 1997) suggests that two-component fits are more appropriate, low-temperature dust at $\sim 50\text{ K}$, presumed to be heated by starburst, and high-temperature dust at $\sim 150\text{ K}$, possibly heated by an AGN; whereas observations of quasars (Haas et al. 1998) suggest much higher ($150\text{ K} \lesssim T_d \lesssim 600\text{ K}$) temperatures for this component. Since the existing $z > 4$ data do not constrain two-component fits, we assume that the 850 μm flux is dominated by the low-temperature component.

The FIR luminosity is obtained by integrating under a single modified blackbody curve. Given, $T_d=50\text{ K}$ and $\beta=1.5$, L_{FIR} is directly proportional to M_d :

$$L_{\text{FIR}} \approx 3.3 \times \left(\frac{M_d}{10^8 M_\odot} \right) \times 10^{12} L_\odot. \quad (3)$$

Assuming that the FIR flux is due to dust heated by a starburst, the star formation rate is given by:

$$SFR = \alpha \times 10^{-10} \frac{L_{\text{FIR}}}{L_\odot} M_\odot \text{ yr}^{-1}, \quad (4)$$

where the value of α depends upon the stellar initial mass function (IMF) adopted and the timescale for the burst. For example, Scoville & Young (1983) deduce $\alpha = 0.77$ by

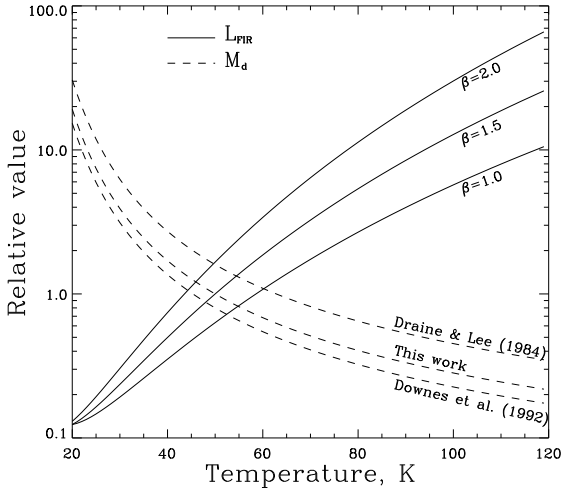


Figure 2. Variation of derived dust mass and FIR luminosity with dust temperature, relative to values with $T = 50$ K and $\beta = 1.5$, for various values of β and absorption coefficient, calculated from a $850 \mu\text{m}$ flux from a dust cloud at $z = 4.5$.

considering the total energy radiated by main sequence O, B and A stars ($M > 1.6 M_{\odot}$), over $\sim 10^9$ yr; whereas Thronson & Telesco (1986) obtain $\alpha = 2.1$, assuming a Salpeter IMF. Allowing for the low mass ($1.6 M_{\odot} > M > 0.1 M_{\odot}$) stars, α rises by a further factor ~ 3 .

Table 2 shows results derived for a sample of cosmological submillimetre sources, in a self-consistent manner, to enable comparison of observed and derived properties. The uncertainties inherent in our assumptions are illustrated in Figure 2. Note that the uncertainties in FIR luminosities reflect solely the uncertainty in the flux, and do not include the uncertainty due to the assumed single temperature. In Figure 3 are plotted the inferred FIR luminosities against optical luminosity for the $z > 4$ quasars. Since the quasar BR1202–0725 has been resolved into two millimetre and optical sources (Omont et al. 1996b; Hu, McMahon & Egami 1996) it is plotted as two discrete points, since its extreme luminosity might be explained if it represents the merger of two gas-rich galaxies or of an AGN and a gas-rich galaxy.

4 DISCUSSION

From the results presented in Figure 3, there is no obvious correlation between L_{FIR} and L_{UV} . Indeed, over a range of a factor of 1.5 in UV luminosity, the scatter in L_{FIR} is ~ 10 . The absence of a strong correlation between L_{FIR} and L_{UV} is supported by the results tabulated in Table 2, with the obvious caveat that this compilation, is rather heterogeneous and consists primarily of detected objects. This conclusion has the implication that the high redshift AGN population may have a FIR luminosity function that is independent of UV luminosity.

In earlier mm/submm work (Isaak et al. 1994; Omont et al. 1996a), only a small fraction (~ 20 percent) of the observed sources were detectable, and the observational limits were at quite high FIR luminosities. These new observations indicate that the typical luminous quasar has a FIR luminosity less than or equal to that of Arp220.

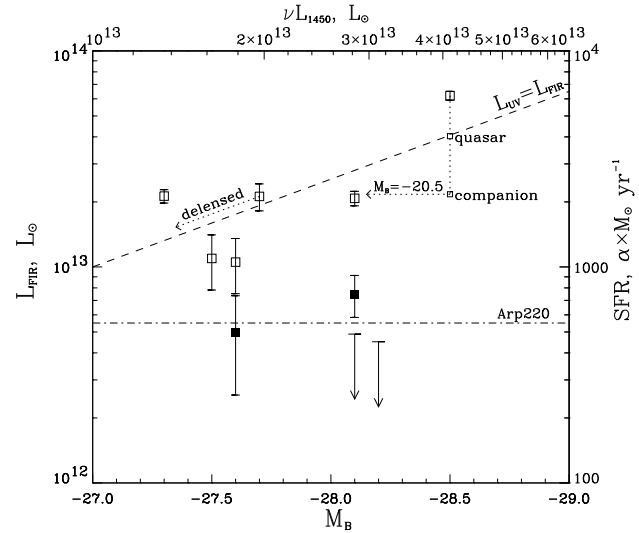


Figure 3. FIR luminosity and inferred star formation rate against absolute B -band magnitude for the $z > 4$ quasars tabulated in Table 2. Filled squares and upper limits: this work. Open squares: previously studied quasars. The dot-dashed horizontal line shows the FIR luminosity of Arp220. The dashed line shows the locus of $L_{\text{FIR}} = L_{\text{UV}}$.

We can investigate the AGN contribution to the deep SCUBA source counts using a simple model where all AGN have a fiducial FIR luminosity of $\sim 5 \times 10^{12} L_{\odot}$ with an Arp220-like spectrum in the submm range. We assign this FIR luminosity to each quasar and adopt a standard Boyle, Shanks & Peterson (1988) quasar luminosity function, extrapolating to high redshifts by assuming no evolution between $z = 2$ and $z = 3$, and a density fall-off by a factor of 2 per unit redshift thereafter. Integrating the luminosity function down to $M_B = -23.0$, we find that there are ~ 140 quasars deg^{-2} . This absolute magnitude limit is primarily based on historical convention from ground based image quality, and if we relax this limit and extrapolate down to $M_B = -21.0$, the source density reaches ~ 400 deg^{-2} . Finally, if one allows for the observed ratio of Seyferts II to Seyferts I at low redshift (2.3 ± 0.7 ; Huchra & Burg, 1992), even neglecting any contribution from totally optically obscured AGN, it is feasible that that a major part (15–100 per cent) of the SCUBA source population could possess AGN.

Further evidence for such high space densities of AGN comes from the deepest X-ray surveys which reach source densities of ~ 1000 deg^{-2} (Hasinger et al. 1998). Whilst the nature of the faintest sources is still controversial, an AGN origin for the energy source is widely considered as the most plausible explanation (*e.g.* Hasinger et al. 1998). Furthermore, estimates of the local space density of massive dark objects within galaxies (Magorrian et al. 1998) exceed the density of the optically-selected quasars, of which these objects are presumed to be the dull remnants (Haehnelt, Natarajan & Rees 1998; Trentham et al. 1998): there may exist a significant population of AGN which are either obscured by dust or accrete in low-efficiency modes.

Lower limits on the contribution of AGN to the submm source counts comes from studies of local ultraluminous infrared galaxies. These limit the fraction of ULIRGs in which AGN activity is the primary energy source to 20–30 percent,

although these observations do not exclude the possibility that the remaining starburst-dominated cases contain AGN as well (Genzel et al. 1998).

An alternative estimate of the contribution of broad line AGN to the submm source counts can be derived by assuming that L_{FIR} is linearly correlated with L_{UV} as shown in Figure 3. Above 3mJy at 850 μ m, the source density ranges between 4 and 9 deg⁻² for a thermal spectrum with temperature of 70K and 30K respectively. This is essentially because only AGN with $M_B < -25$ would have detectable flux at 850 μ m. It is thus important that observations of quasars with $M_B < -25$ are carried out at 850 μ m to distinguish between the range of models.

If AGN are present in a significant fraction of the SCUBA sources, this has important implications for studies which use the SCUBA source counts to infer star formation rates from the from a 850 μ m flux. The tacit assumption in Equation 3 is that this locally-derived relation between L_{FIR} and the star formation rate, based on galaxies such as M51 in which $L_{FIR} \sim 10^{10} L_{\odot}$, can be applied within the extreme environments of high redshift AGN and massive starbursts, in which FIR luminosities are 100–1000 times larger. For example, the intense UV flux from any starburst or AGN could suppress the formation of low mass stars which dominate the total mass. Thus, even if the dust is not heated by a more energy-efficient AGN, the AGN's presence may effect the underlying IMF which is used to deduce the total star formation rate.

5 CONCLUSIONS

We have observed a small but statistically-complete sample of luminous high redshift ($z > 4$) quasars with SCUBA at 850 and 450 μ m, and have found that the typical FIR luminosity of these quasars is less than or comparable with that of the archetypal local ultraluminous IRAS galaxy Arp220. Using a simple model for the contribution of AGN to the submm source population, we find that $\gtrsim 15$ per cent of the sources in the deep SCUBA surveys at the $S_{850} \sim 3\text{--}4\text{mJy}$ level, may contain active nuclei. Hence, both the contribution of AGN to the FIR luminosity, and its effect upon the underlying IMF (should starburst be the dominant power source), need to be considered.

Further submm studies of lower redshift and lower luminosity quasars are required in order to determine directly the far infrared luminosity function for quasars. In addition sensitive X-ray observations with *AXAF* and *XMM* may determine the fraction of the SCUBA sources which harbour AGN.

ACKNOWLEDGMENTS

We thank Kate Isaak and the referee for comments which helped us clarify the contents of this paper. RGM thanks the Royal Society for support, and RSP acknowledges receipt of a PPARC studentship. IS acknowledges support under the European Commission, TMR Programme, Research Network Contract ERBFMRXCT96-0034 "CERES". The JCMT is operated by the Joint Astronomy Center on behalf

of the UK Particle Physics and Astronomy Research Council, the Netherlands Organisation for Scientific Research and the Canadian National Research Council.

REFERENCES

- Barger, A.J., Cowie, L.L., Sanders, D.B., Fulton, E., Taniguchi, Y., Sato, Y., Kawara, K., Okuda, H., 1998, *Nature*, 394, 248
 Barnes, J.E., & Hernquist, L., 1996, *ApJ*, 471, 115
 Becker, R.H., White, R.L., Helfand, D.J., 1995, *ApJ*, 450, 559
 Boyle, B.J., Shanks, T., & Peterson, B.A., 1988, *MNRAS*, 235, 935
 Carico, D.P., Keene, J., Soifer, B.T., Neugebauer, G., 1992, *PASP*, 104, 1086
 Condon, J.J., Cotton, W.D., Greisen, E.W., Yin, Q.F., Perley, R.A., Taylor, G.B., 1998, *AJ*, 115, 1693
 Downes, D., Solomon, P.M., Radford, S.J.E., 1995, *ApJ*, 453, L65.
 Draine, B.T., Lee, H.M., 1984, *ApJ*, 285, 89
 Dunlop, J.S., Hughes, D.H., Rawlings, S. Eales, S. & Ward, M., 1994, *Nature*, 370, 347
 Eales, S., Lilly, S., Gear, W., Dunne, L., Bond, J.R., Hammer, F., Le Fèvre, O., Crampton, D., 1998,
 Eisenhardt, P.R., Armus, L., Hogg, D.W., Soifer, B.T., Neugebauer, G., Werner, M.W., 1996, *ApJ*, 461, 72
 Genzel, R., et al., 1998, *ApJ*, 498, 579
 Green, S.M. & Rowan-Robinson, M. 1996, *MNRAS*, 279, 884
 Haehnelt, M., & Rees, M.J., 1993, *MNRAS*, 263, 168
 Haehnelt, M., Natarajan, P., & Rees, M.J., 1998,
 Haas, M., Chini, R., Meisenheimer, K., Stickel, M., Lemke, D., Klaas, U., Kreysa, E., 1998, *ApJ*, 503, L109
 Hasinger, G. et al., 1998, *A&A*, 329, 482
 Hildebrand, R.H., 1983, *QJRAS*, 24, 268
 Holland, W.S., Cunningham, C.R., Gear, W.K., Jenness, T., Laidlaw, K., Lightfoot, J.F., Robson, E.I., submitted to *MNRAS*, 1998, astro-ph/9809122
 Hooper, E.J., Impey, C.D., Foltz, C.B., Hewett, P.C, 1995, *ApJ*, 445, 62
 Hu, E.M., McMahon, R.G., & Egami, E., 1996, *ApJ*, 459, L53
 Huchra J., Burg, R., 1992, *ApJ*, 393, 90
 Hughes, D.H., Dunlop, J.S., Rawlings, S., 1997, *MNRAS*, 289, 766
 Hughes, D.H., et al., 1998, *Nature*, 394, 241
 Isaak, K.G., McMahon, R.G., Hills, R.E., Withington, S., 1994, *MNRAS*, 269, L28
 Ivison, R.J., et al., 1998, *ApJ*, 494, 211
 Ivison, R.J., Smail, I., Le Borgne, J.-F., Blain, A.W., Kneib, J.-P., Bézecourt, J., Kerr, T.H., Davies, J.K., 1998b, *MNRAS*, 298, 583
 Klaas, U., Haas, M., Heinrichsen, I., Schulz, B., 1997, *A&A*, 325, L21
 Lewis, G.F., Chapman, S.C., Iбата, R.A., Irwin, M.J., Totten, E.J., 1998, Preprint astro-ph/9807293
 Magorrian, J., et al., 1998, *AJ*, 115, 2285
 McMahon R.G., Omont A., Bergeron J., Kreysa E., Haslam C.G.T., 1994, *MNRAS*, 267, L9
 Omont, A., McMahon, R.G., Cox, P., Kreysa, E., Bergeron, J., Pajot, F., Storrie-Lombardi, L.J., 1996a, *A&A*, 315, 1
 Omont, A., Petitjean, P., Guilloateau, S., McMahon, R.G., Solomon, P.M., Pécontal, E., 1996b, *Nature*, 382, 428
 Rowan-Robinson, M., et al., 1993, *MNRAS*, 261, 513
 Scoville, N.Z., & Young, 1983, *ApJ*, 265, 148
 Smail, I., Ivison, R.J., Blain, A.W., 1997, *ApJ*, 490, L5
 Storrie-Lombardi, L.J., McMahon, R.G., Irwin, M.J., Hazard, C., 1996, *ApJ*, 468, 121
 Thronson, H., & Telesco, C., 1986, *ApJ*, 311, 98
 Trencham, N et al, 1998, astro-ph/9812081

Yun, M. S., Scoville, N. Z., Carrasco, J.J., Blandford, R. D., 1997,
ApJ, 479, L9